

Time stretch and its applications

Ata Mahjoubfar^{1,2}, Dmitry V. Churkin^{3,4,5}, Stéphane Barland⁶, Neil Broderick⁷, Sergei K. Turitsyn^{3,5}
and Bahram Jalali^{1,2,8,9*}

Observing non-repetitive and statistically rare signals that occur on short timescales requires fast real-time measurements that exceed the speed, precision and record length of conventional digitizers. Photonic time stretch is a data acquisition method that overcomes the speed limitations of electronic digitizers and enables continuous ultrafast single-shot spectroscopy, imaging, reflectometry, terahertz and other measurements at refresh rates reaching billions of frames per second with non-stop recording spanning trillions of consecutive frames. The technology has opened a new frontier in measurement science unveiling transient phenomena in nonlinear dynamics such as optical rogue waves and soliton molecules, and in relativistic electron bunching. It has also created a new class of instruments that have been integrated with artificial intelligence for sensing and biomedical diagnostics. We review the fundamental principles and applications of this emerging field for continuous phase and amplitude characterization at extremely high repetition rates via time-stretch spectral interferometry.

The Shannon–Hartley theorem provides a tool to quantify the information content of analog data. The theorem prescribes that unpredictability — the element of surprise — is the property that defines information. No information is carried by a periodic signal, such as a sinusoidal wave, because its evolution is entirely predictable. Conversely, events that are rare and random convey a large amount of information as their arrival was not expected by the observer.

Such occurrences of random events contain precious information about systems that produce them¹. Also known as outliers and black swans², these phenomena appear in complex dynamic systems such as hydrodynamics, plasma physics, nonlinear optics and financial markets. In this context, chaos is another example of random processes that emerge in complex systems and offers a wealth of information about the underlying nonlinear system and its interaction with its surroundings.

Detection of rare events and non-stationary processes in ultrafast electronic and optical systems imposes daunting technological challenges. To detect fast events whose time of arrival are unknown, the instrument must have fine temporal resolution and long record lengths. It needs to resolve the fast (intrapulse) timescale as well as the slow (interpulse) timescale spanning trillions of sequential pulses. These requirements cannot be met by temporal reconstruction via pump–probe techniques as they operate in equivalent-time (similar to a strobe light) rather than in real time. A new generation of instruments based on photonic time stretch is opening the path to measuring and understanding the behaviour of non-stationary and rare phenomena in ultrafast systems, and harvesting their potential for practical applications such as metrology, machine vision and biomedicine. While these instruments rely on optics for the transformation of a signal's timescale, they are able to operate with either electrical, optical, or terahertz inputs.

The development of spectroscopy by Kirchhoff and Bunsen in the mid-nineteenth century unveiled the quantized nature of atomic radiation that led to the development of quantum theory. The history of science consists of a number of such episodes where breakthroughs

in instrumentation have led to new science. We anticipate that a new type of instrument that performs time-resolved single-shot measurements of ultrafast events and that makes continuous measurements over long timescales spanning trillions of pulses will unveil previously unseen physical phenomena leading to advances in applications and understanding of complex systems.

Challenges with current systems

Optical systems are characterized by their spectral and temporal responses. Conventional tools for measurement of laser spectra (for example, optical spectrum analysers) only capture data averaged over a considerable time period. Standard spectroscopy relies on well-developed mechanically scanning or imaging techniques³. However, the achievable scanning rate (or frame rate) is usually too slow, often by many orders of magnitude, to resolve the fast spectral dynamics of laser systems⁴ such as soliton complexes. The same limitation also prevents the use of conventional spectrometers for the study of rare events, such as optical rogue waves and probabilistic soliton dynamics, a field that has been rapidly growing since its inception in 2007^{5–10}. In such a nonlinear dynamic system, a wealth of information can be obtained from the capture and digital analysis of non-repetitive spectra generated by noise or chaotic dynamics. However, owing to the spontaneous occurrence and non-cyclical nature of rogue events, traditional pump–probe techniques fail to capture them. The problem is further exacerbated by the rarity of their appearance, which requires long and continuous recording in addition to fast real-time operation.

The difficulty in fast real-time measurements

There are two fundamental challenges with any fast real-time optical measurement¹. The first is the limitation of the data converter, that is, the trade-off between the dynamic range (measured in number of bits) and the speed of the real-time analog-to-digital converter (ADC; the digitizer). The second is the trade-off between the speed and the sensitivity of the optoelectronic front-end. High speed comes at the

¹Department of Electrical Engineering, University of California, Los Angeles, California 90095, USA. ²California NanoSystems Institute, Los Angeles, California 90095, USA. ³Aston Institute of Photonic Technologies, Aston University, Birmingham B4 7ET, UK. ⁴Institute of Automation and Electrometry, Siberian Branch of the Russian Academy of Sciences, Novosibirsk 630090, Russia. ⁵Novosibirsk State University, Novosibirsk 630090, Russia.

⁶Universite de Nice - CNRS UMR 7335, Institut Non Lineaire de Nice, 1361 Route des Lucioles 06560, Valbonne, France. ⁷Dodd Walls Centre for Photonic and Quantum Electronics, Department of Physics, The University of Auckland, Private Bag 92019, Auckland 1142, New Zealand. ⁸Department of Bioengineering, University of California, Los Angeles, California 90095, USA. ⁹Department of Surgery, David Geffen School of Medicine, University of California, Los Angeles, California 90095, USA. *e-mail: jalali@ucla.edu

Box 1 | Nominal versus effective number of bits of a digitizer.

The performance of an ADC cannot be specified by its nominal (physical) bit-depth. In most ADCs, the last few bits of the digital value are inaccurate due to the noise and distortion. Therefore, a characteristic measure named effective number of bits, ENOB, is defined to indicate the number of meaningful bits. ENOB at an analog input frequency can be measured as

$$\text{ENOB} = \frac{10 \times \log_{10} \left(\frac{P_{\text{signal}}}{P_{\text{noise}} + P_{\text{distortion}}} \right) - 1.76}{6.02}$$

where P_{signal} , P_{noise} and $P_{\text{distortion}}$ are the signal, noise and distortion powers, respectively. Also, it is assumed that the input signal amplitude matches the full-scale range of the ADC input. Generally, ENOB decreases at higher frequencies.

price of low sensitivity because few photons are collected during the short integration time¹¹.

The most successful non-electronic method to alleviate the ADC speed limitations has been the photonic time-stretch technology, which slows down the signal prior to digitization^{12–14}. This technology has led to the discovery of optical rogue waves⁵, inspection of other noise-driven ultrafast dynamics such as fibre soliton explosions¹⁵, observation of internal motions of soliton molecules¹⁶ and relativistic electron structures in accelerators^{17,18}, characterization of noise-induced fluctuations in gain spectrum¹⁹, and single-shot stimulated Raman spectroscopy of biochemicals^{20,21}. Recently, label-free classification of cancer cells in blood has been achieved using time-stretch spectral interferometry augmented with artificial intelligence and big-data analytics²². Further advances in the form of warped (anamorphic) stretch can engineer the time–bandwidth product of the signal envelope^{e23–25}, with direct utility in foveated (non-uniform) sampling for improvement of data acquisition rate²⁶, optical data compression²⁷, enhancement of signal-to-noise ratio and feature detection²⁸.

The second problem of an insufficient number of collected photons during fast real-time measurement is solved by distributed amplification implemented using stimulated Raman scattering within the same optical element where time stretch occurs (typically a dispersive fibre). Alternatively, a discrete amplifier can be used. The amplified time-stretch technique was originally developed to enable real-time analog-to-digital conversion with femtosecond resolution²⁹, and later was applied to a variety of time-stretch instruments for spectroscopy¹⁹ and imaging^{30–33}.

Here, we review photonic time-stretch technology and discuss its use in data acquisition and data analytics for the measurement and characterization of rare events in the context of electronic signals, spectroscopy and imaging. Finally, the newest developments including the combination of time-stretch instruments with artificial intelligence and machine learning for data capture and classification are examined.

Fundamentals of time stretch

In this section, we describe the fundamental challenge in single-shot continuous measurements posed by the ADC and describe how it can be overcome with time stretch. We also describe various realizations of group delay dispersion used to implement linear and warped-stretch transformations.

ADC limitations and improvement by time stretch. ADCs measure the amplitude of a continuous-time signal at periodic time intervals and round the measurement value to a set of digital numbers

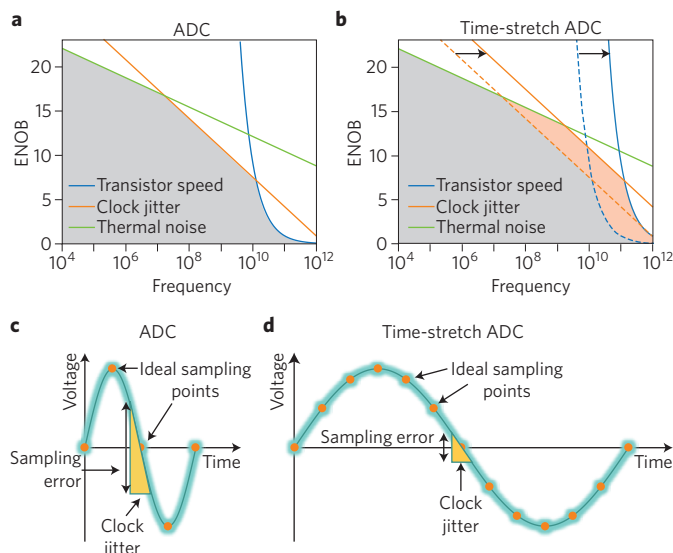


Figure 1 | Digitizer bottlenecks and solutions via time stretch. As the sampling rate of an analog-to-digital converter (ADC) increases, its dynamic range, measured by the effective number of bits (ENOB), reduces. Three factors are responsible for this: comparator ambiguity caused by the limited gain bandwidth of the transistors, sampling error due to the clock jitter (known as aperture jitter), and thermal (Johnson) noise of the electronic components. **a**, Among these, the comparator ambiguity and the aperture jitter are the dominant performance-limiting factors at high speeds. **b**, By slowing down the signal, time stretch resolves these issues by suppressing the effect of the aperture jitter and the comparator ambiguity¹⁴. **c,d**, Consider a high-frequency signal being sampled directly by an ADC. A small jitter will cause a significant error in the sampled amplitude (**c**), whereas if the signal is slowed down by time stretch prior to the sampling, the effect of clock jitter is considerably reduced (**d**). Also, slowing down the signal relaxes the comparator speed requirements. Time-stretch ADC works on burst data, but also on continuous data using a technique known as virtual time gating⁴⁹.

specified by the bit depth. The process of measurement at specific time points is known as sampling. The rounding operation, also called quantization, is implemented by comparators that associate the analog amplitude with a set of reference levels. Depending on the speed and accuracy requirements, ADCs are designed with different architectures and contain a various number of sample-and-hold blocks and quantizers. Because precision of the sampling times and the quantization levels directly influence the performance, many designs utilize additional circuitry for stable sampling clock generation and for digital calibration.

Because an ADC approximates an analog value to a discrete number of digital levels, it inevitably introduces an error. This error appears as a noise source referred to as quantization noise, the amount of which depends on the nominal bit depth. However, there are other non-idealities that reduce the effective bit depth and prevent reaching the nominal value (Box 1). Among them, the most fundamental are thermal noise, comparator switching speed that causes ambiguity in the quantized level, and jitter of the sampling clock (Fig. 1). The performance of the ADCs designed for low frequencies is often limited by the aggregate thermal noise. For high-speed data converters, the gain bandwidth of the transistor technology causes ambiguity in the amplitude. Also limiting the performance of high-speed digitizers is the aperture jitter that is caused by the phase noise of the sampling clock or the timing skews rooted in mismatches between different channels in parallel architectures.

By slowing down the analog signal before the digitizer, time stretch addresses the sampling jitter and the comparator ambiguity problems, while thermal noise remains unchanged^{28,34,35}. Also, it brings

other intrinsic benefits of optics to the data converter such as low-jitter optical clocks formed by mode-locked lasers^{36–38}, high bandwidth, negligible crosstalk and immunity to electromagnetic interference. In a recent demonstration of a time-stretch ADC, the aperture jitter is reduced from 270 fs to 20.5 fs, a 13-fold jitter suppression³⁹.

Photonic time-stretch data acquisition. This technology consists of four steps (Fig. 2). In step 1, the information is modulated onto the optical spectrum. When the starting information is a temporal waveform, this step consists of electro-optical or all-optical modulation of the information onto a broadband, chirped optical carrier. For imaging applications, this step is spectral encoding of the target onto a broadband pulse via illumination with a rainbow (spatially dispersed broadband pulse). For spectroscopy, the desired information is already present in the spectrum so this step is not necessary and can be viewed as modulation with a unity transfer function. In step 2, the information residing in the spectrum is stretched in time by means of a natural or synthetic dispersive element (Fig. 3). In step 3, the optical signal is photodetected and digitized using a real-time data converter. Coherent detection via spectral interferometry is employed when signal phase, in addition to its amplitude (full-field) is required. Step 4 consists of digital signal processing and data analytics such as machine learning for classification of the captured data²². These four steps of a time-stretch system resemble an optical data communication link consisting of modulation by the transmitter (step 1), propagation in a channel, albeit a dispersive channel (step 2), detection by the receiver (step 3) and data processing in higher layers of the communication link (step 4). The combination of time stretch functioning as a photonic hardware accelerator with parallel data processing via

graphics processing units, field-programmable gate arrays, or tensor processing units (TPU) plus novel artificial-intelligence algorithms optimized for high-performance computing opens up a new frontier in real-time metrology, sensing and imaging.

In step 2, distributed Raman amplification is induced in the dispersive fibre to overcome the intrinsic loss caused by reduction of peak power from temporal spreading of energy, and to compensate for extrinsic loss due to fibre and component losses. With other types of dispersive element, such as a chirped fibre Bragg grating or a chromomodal dispersion device (Fig. 3), a lumped element amplifier is placed before the dispersive element to overcome its losses. The high sensitivity of the time-stretch system is partially due to the use of distributed optical amplification but also because the system does not rely on nonlinear optical interaction. The resolution of the spectral measurement is set by the maximum amount of dispersion that can be employed (equation (6) in Box 2). However, larger dispersion comes at the expense of higher loss.

As shown in Fig. 3, there are several device options for implementing the group delay dispersion in step 3 of the time-stretch system. These devices can generate both linear dispersion for the classical time stretch and nonlinear dispersion for warped (foveated) stretch. The latter has been used for optical data compression via non-uniform Fourier domain sampling, whereby information-rich portions of the spectrum are sampled at a higher density than sparse regions, leading to the concept of the analog information gearbox^{26,28,40}. One practical approach to creating large amounts of nonlinear dispersion with arbitrary frequency dependency is by using an arrayed waveguide grating in a feedback configuration known as the recirculating photonic filter⁴¹ (Fig. 3c).

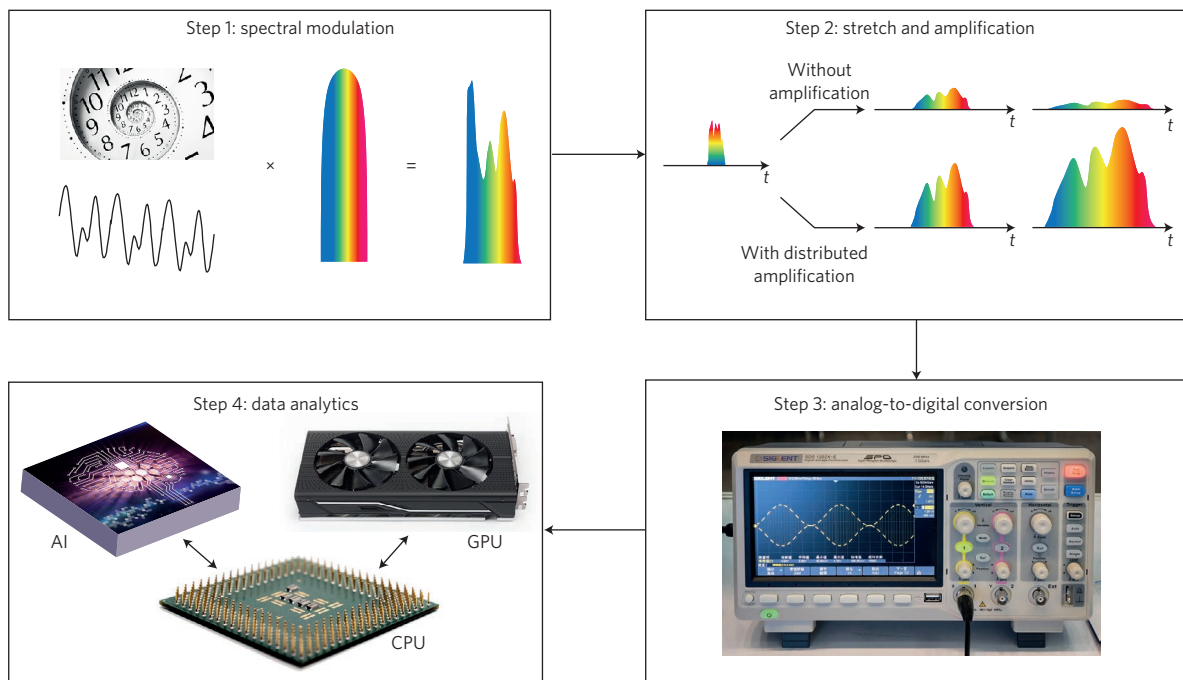


Figure 2 | Building blocks of a time-stretch system. A photonic time-stretch system consists of four steps. Step 1: an input signal along with the information carried by it is modulated onto the spectrum of wideband ultrashort optical pulses. Step 2: a group delay dispersive element spreads the spectral components in time causing the information modulated onto the spectrum to be slowed down. This relaxes the speed requirement of the ADC and enhances the digitizer performance as described in Fig. 1. Depending on the amount of dispersion used and the optical bandwidth of the input, this dispersive transformation can be in the near- or far-field. The so-called time-stretch dispersive Fourier transform (TS-DFT) occurs in the far-field regime where the amount of dispersion is large enough to satisfy the stationary phase approximation. Step 3: the optical signal is converted to an analog electrical waveform through photodetection, and then digitized by a real-time ADC. Step 4: digital data analysis and classification using artificial intelligence (AI) is performed in a central processing unit (CPU) or a dedicated processor such as a graphics processing unit (GPU). Images: infinite spiral clock, liseykina / iStock / Getty Images Plus; oscilloscope, RaymondAsiaPhotography / Alamy Stock Photo; AI, Alexey Kotelnikov / Alamy Stock Photo; CPU, Petr Bonek / Alamy Stock Photo; GPU, Patrik Slezak / Alamy Stock Photo.

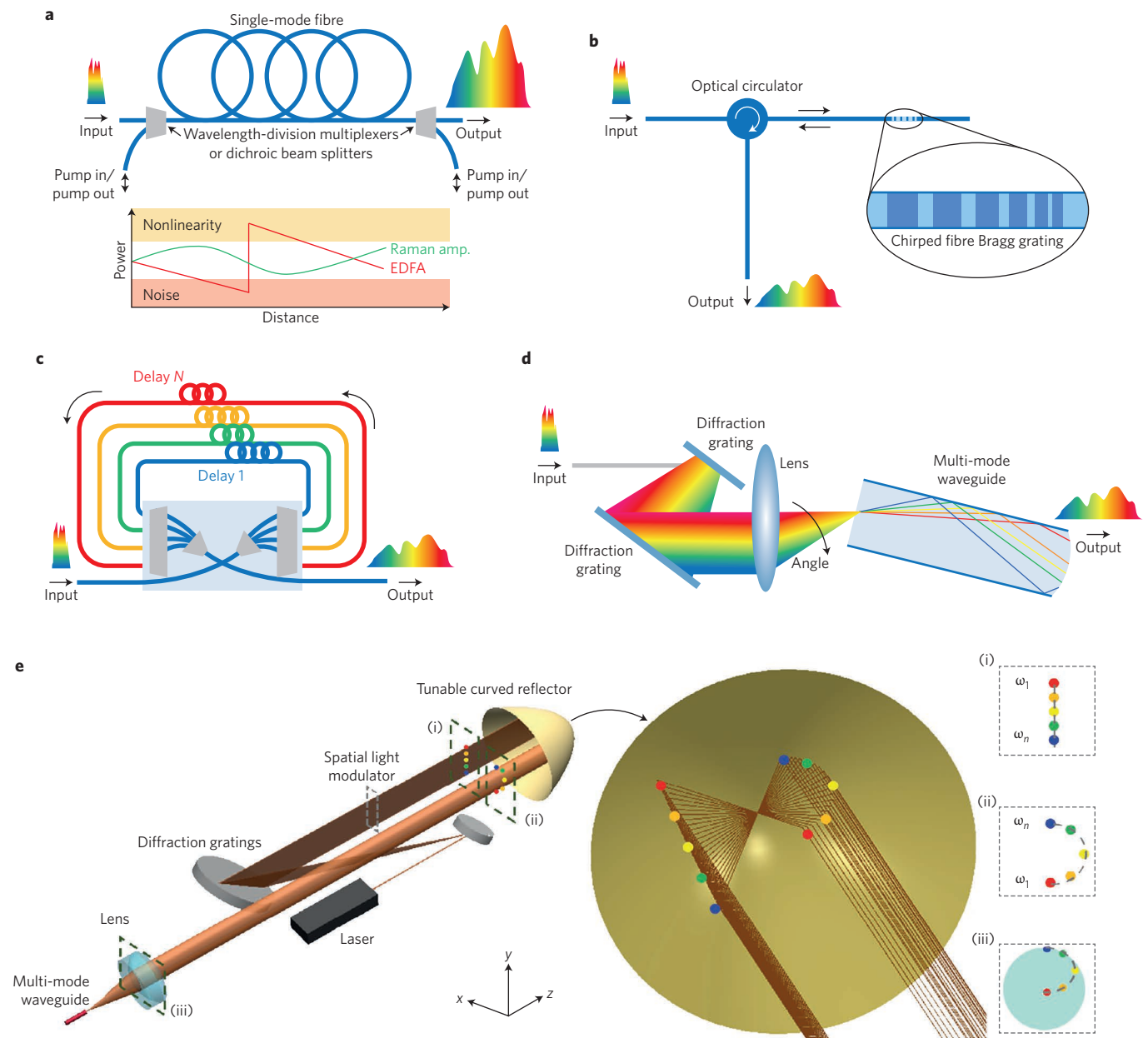


Figure 3 | Different dispersion devices. Group delay dispersion used in time stretch can be experimentally realized using a number of different device designs. **a**, An optical fibre with internal Raman amplification provides high dispersion combined with net gain. The pump power is gradually transferred to the signal (Stokes wavelength) avoiding noise (low-power) and nonlinear (high-power) regions. EDFA, erbium-doped fibre amplifier. **b**, Chirped fibre Bragg grating is advantageous at implementing arbitrary group delay profiles. **c**, A different approach is a recirculating photonic filter using an arrayed waveguide grating in which an arbitrary delay is applied to each spectral channel⁴¹. **d**, Spectral-to-angular-to-temporal mapping (chromomodal dispersion device) exploits the large modal dispersion of a multi-mode waveguide (a fibre or a pair of planar reflectors) to achieve extremely high chromatic dispersion at 800 nm or visible bands where dispersive fibres are not available¹²². **e**, Chromomodal dispersion can be extended to synthesize nonlinear group delay profiles using curved reflectors (middle) to warp the spectro-angular profile (from (i) to (ii)), and then radially transform and map this nonlinear profile into angular excitation of the modes of a multi-mode waveguide (iii)²⁸. Panels **a,b,d,e** adapted from ref. 28, IEEE.

With sufficient dispersion satisfying the stationary phase approximation, the spectrum is mapped into the time domain that, in the case of linear dispersion, results in the classical time-stretch dispersive Fourier transform (TS-DFT). This far-field regime of temporal dispersion (TS-DFT) is a special case of the general time-stretch transform. The general form also includes the near-field regime, where both intensity and phase are used for the reconstruction of the input waveform. Such full-field real-time measurements can be realized using phase retrieval from intensity measurements⁴², or with coherent detection^{31,43}. While the stretch factor achieved in the near field is smaller

than that in the far field, in many cases, the smaller factor is sufficient to overcome the key problem of the ADC speed bottleneck. Therefore, it is important to note that even though achieving a Fourier transform simplifies signal reconstruction and interpretation, it does not enable fast real-time measurements. The ability to slow down the waveform's timescale is what overcomes the critical ADC speed bottleneck.

Common methods for the characterization of ultrafast optical pulses such as frequency-resolved optical gating (FROG)⁴⁴ and spectral phase interferometry for direct electric-field reconstruction (SPIDER)⁴⁵ are proven and successful laser-pulse-characterization

Box 2 | Time-stretch spectral shearing interferometry for full-field measurements.

Time stretch can be readily analysed by modelling the band-pass optical signals with low-pass complex envelopes. The transfer function of the dispersive element in the time-stretch system, $H(\omega)$, is mainly a phase propagator:

$$H(\omega) = e^{i\phi(\omega)} = e^{i\sum_{m=0}^{+\infty} \phi_m(\omega)} = \prod_{m=0}^{+\infty} H_m(\omega) \quad (1)$$

in which $\phi(\omega)$ is the phase profile of the group delay dispersion²⁸, and its range can reach 10^6 radians. $\phi_m(\omega)$ are the phase modes resultant from the expansion of the phase function space in a basis set. The transfer function can be viewed and implemented as a cascade of mode operators, $H_m(\omega)$. The group delay profile of this propagator, $\tau(\omega)$, is

$$\tau(\omega) = \frac{d\phi}{d\omega} = \sum_{m=1}^{+\infty} \tau_m(\omega) \quad (2)$$

where $\tau_m(\omega)$ are the group delay modes of the cascaded operators.

Assuming the optical carrier frequency is at ω_c , the down-converted spectrum of an optical pulse with complex envelope $E_c(t)$ is denoted by $\tilde{E}_i(\omega = \omega_c - \omega)$, where ω_c is the optical frequency and ω is the modulation frequency. On propagation through the time-stretch system, the pulse is reshaped into a temporal signal with a complex envelope given by

$$E_o(t) = \frac{1}{2\pi} \int_{-\infty}^{+\infty} \tilde{E}_i(\omega) H(\omega) e^{i\omega t} d\omega \quad (3)$$

Using stationary phase approximation, which is satisfied when filter group delay is relatively large leading to the far-field regime of dispersion, only the frequency component ω contributes to the signal at time t according to the relation $t = \tau(\omega)$ and equation (3) is estimated as

$$E_o(t) \propto \tilde{E}_i(\omega = \tau^{-1}(t)) \quad (4)$$

which means the spectrum is mapped to time with the group delay profile. $\tau^{-1}(t)$ is the inverse function of the mapping described by

equation (2), and it can be nonlinear. Only if the group delay profile is linear, $\tau(\omega) = \tau_0' \omega + \tau_0$ (the group delay dispersion is constant), equation (4) is simplified as

$$E_o(t) \propto \tilde{E}_i\left(\omega = \frac{t - \tau_0}{\tau_0'}\right) \quad (5)$$

where τ_0 is the time of arrival at the photodetector for the carrier frequency, ω_c , and the mapping of the spectrum to time is uniform. This is the regime called time-stretch dispersive Fourier transform (TS-DFT). The spectral resolution, corresponding to the ambiguity in frequency-to-time mapping^{26,126}, is approximately

$$\delta\omega(\omega) = \sqrt{\frac{4\pi}{\left|\frac{d\tau(\omega)}{d\omega}\right|}} \quad (6)$$

Resolution scales inversely with the amount of group delay dispersion. In coherent time stretch (also known as time-stretch spectral interferometry), an interferometer splits the pulse into two arms with delay of τ_d with respect to each other. Once these two copies of the pulse are recombined, an interference pattern is formed in the output of the interferometer, which embeds the pulse phase information:

$$|E_o(t)|^2 \propto |\tilde{E}_i(\omega_1)|^2 + |\tilde{E}_i(\omega_2)|^2 + 2|\tilde{E}_i(\omega_1)||\tilde{E}_i(\omega_2)|\cos(\Delta\phi + (\omega_1 - \omega_2)t) \quad (7)$$

in which, $\omega_1 = \tau^{-1}(t)$, $\omega_2 = \tau^{-1}(t - \tau_d)$, and the difference of the input pulse phases at these two frequencies is contained in $\Delta\phi$, forming time-stretch adaptation of spectral shearing interferometry. The time-stretch interferogram can be captured by an ADC, providing complex field acquisition in single shot, but in a continuous fashion. The accuracy of the complex field measurement would be bound by the spectral resolution given by equation (6) and by the ENOB of the ADC.

techniques. A common feature of both methods is the reliance on nonlinear optical interactions. FROG uses a nonlinear medium to gate the electric field of an optical pulse with its own intensity. The optical field is gated at different time delays and captured by a spectrometer, resulting in a spectrogram. As long as the time windows of the gated measurements overlap, the spectrogram implicitly contains the phase information, and an iterative algorithm can recover the optical pulse phase and intensity from the spectrogram. On the other hand, SPIDER uses the nonlinear medium to mix two copies of the input pulse with a chirped pulse as the source of spectral shear. The chirp pulse is generated from the input pulse itself by dispersing it in time until its frequency components are separated. The difference in frequency shift of the copies results in a beating pattern (fringes) in the spectrum, which is the basis of spectral shearing interferometry. The optical pulse phase can be derived from this spectral interferogram. Another novel technique is based on the measurement of power spectra before and after propagation of the pulse through a nonlinear fibre followed by an iterative algorithm⁴⁶.

All three methods are excellent tools for laser pulse characterization, but because of their reliance on nonlinear optical interactions, they may not be ideal for sensing and metrology applications, where weak signals must be detected. Also, the use of a conventional optical spectrometer limits their continuous real-time operation at high speed, hindering their ability to detect rare events (this issue can be

resolved by the time-stretch spectrometer). The use of complex recovery algorithms may also challenge continuous-time operation in signal acquisition and metrology.

Time-stretch spectral interferometry, also known as coherent time stretch, directly captures the phase and intensity of the optical pulses without relying on nonlinear optical interactions. The system has been developed for high-speed imaging vibrometry³¹, full-field gas spectroscopy⁴⁷ and label-free flow cytometry^{22,48}. Recently, it was used to capture real-time dynamics of soliton molecules¹⁶. In these works, the relative phase of optical pulses was measured. Measurement of absolute phase performed by other techniques described above is more challenging. Time-stretch spectral shear interferometry (Box 2) offers a path for absolute phase measurements.

Time-stretch systems are often used in burst-mode regime, but continuous-time operation is also possible and has been demonstrated⁴⁹⁻⁵². In the continuous-time mode, a virtual time gate is employed to form parallel measurement channels, each acquiring part of the temporal waveform⁴⁹.

Applications

In this section, we describe various applications spanning digital data processing, characterization of optical fluctuations and discovery of new soliton phenomena, optical data compression via foveated sampling affected by warped stretch as well as the integration

of time-stretch data acquisition with machine learning for biomedical applications.

Wideband ADC and digital processing. Originally developed to overcome the ADC speed–accuracy trade-off^{2,13}, photonic time stretch has spawned numerous variations where wideband electronic or optical temporal data are subjected to analog slow-motion processing to enable real-time digital capture and digital processing^{39,51–57} (Fig. 4). Taking advantage of its ability to mitigate noise caused by the sampling clock jitter and ambiguity caused by the finite speed of electronic comparators, time stretch has led to the demonstration of an ADC with the highest speed and dynamic range combination among any ADC technology⁵¹.

Acting as a hardware accelerator, time stretch can enhance the speed of digital processors, such as field-programmable gate arrays or graphics processor units, for real-time sensing and monitoring of ultrahigh-speed data. As a case in point, optical networks must be able to monitor data transmission quality at all times and be able to direct traffic as needed. For this purpose, fast digital processors are essential, however, they are exceedingly power hungry. The time-stretch accelerated processor combines an optical front-end with a digital processor to monitor quality of data transmission in optical networks in real time⁵⁸. It achieves burst-mode digital processing speeds exceeding one terabit per second with a single processor for real-time monitoring of data in the Internet backbone. Reducing the required clock speed of both the digitizer and the processor, the time-stretch hardware accelerator offers superior scaling of power dissipation in the electronic front-end³⁵. Future applications include photonic Internet protocol routing⁵⁹ and optical code division multiple access (CDMA)⁶⁰.

Characterization of noise and fluctuations. The study of noise and fluctuations in nonlinear optics is a fast-growing and high-impact field. Spontaneously generated fluctuations not only set the limit for optical data detection, but also contain a wealth of information about the underlying physics and behaviour of complex dynamic systems. Owing to their non-stationary nature and short timescales, such measurements require a real-time recording system with time resolution in the pico- and femtosecond regimes and long record lengths. Motivated by its success in unveiling previously unseen spectral and temporal phenomena, such as optical rogue waves⁵ and stochastic behaviour in supercontinuum generation⁶¹, it has been suggested that the time-stretch technique “should become the standard method for study of noise and noise driven nonlinear dynamics in optics, the characterization of quantum-optical intensity-correlations in soliton dynamics, and in the study of spectral instabilities in ultrafast nonlinear optics”⁶².

Complex dynamics originate from the interplay of noise and nonlinearities and generate fascinating non-cyclical and rare spectral features. Being able to capture single-shot spectra with continuous recording over trillions of pulses allows researchers to study fluctuations in different regions of the spectrum. The time-stretch spectrometer applied to modulation instability shows that statistical distribution of fluctuations can vary widely ranging from near-Gaussian distribution in the short-wavelength regime to heavy-tail (extreme-value) distributions at long wavelengths^{62,63}. Such wavelength-resolved noise characterization can revolutionize development of low-noise supercontinuum sources for metrology and microscopy. Exploiting the wideband nature of optical dispersion, such statistical studies of a supercontinuum can be carried out over an octave of bandwidth, providing unparalleled utility in understanding and optimization of coherent white-light sources⁶⁴.

Discovery of previously unseen soliton phenomena. Until 2007, extreme-value phenomena were generally not associated with the field of optics. While studying real-time dynamics of supercontinuum generation in photonic crystal fibres, it was observed that extremely rare and random flashes of coherent light are generated at input

power levels below the threshold for a supercontinuum⁵. Utilizing the time-stretch spectrometer’s ability to capture single-shot events with continuous recording over a very large number of events, the statistics of these events was constructed showing heavy-tail (L-shape) distributions in which outliers occur much more frequently than expected from Gaussian statistics. Such unusual distributions describe the probabilities of freak ocean waves and other fascinating phenomena in the physical and social sciences^{2,65–70}. The term optical rogue wave was created to draw attention to statistical similarities to the ocean waves and to the fact that nonlinear optical pulse propagation shares similar mathematics to water waves (both can be described using the nonlinear Schrödinger equation). In this context, photon economics¹ and financial rogue waves⁷¹ capture the parallel between optical and financial systems — both being noise-driven nonlinear systems. Originating from quantum fluctuations via spontaneous emission, optical rogue waves are truly unpredictable, a property not shared by many other extreme-value phenomena because of their classical origin⁷². The ability to collect extensive datasets has created fertile ground for the theoretical study of these noise-driven nonlinear interactions, resulting in new insights in complex systems⁸.

Another experimental milestone is the observation of fibre soliton explosions¹⁵. Soliton explosions is a dissipative phenomenon that can occur in mode-locked lasers⁷³. A soliton in the laser cavity can unexpectedly collapse, only to reappear within a small number of cavity round trips. Originally identified in studies with the complex cubic–quintic Ginzburg–Landau equation⁷⁴, soliton explosions have been difficult to observe experimentally due to their transient appearance. Recently, the time-stretch technique has been employed to observe soliton explosions in single-shot measurements of the spectra of numerous consecutive pulses in the output of a Yb-doped mode-locked fibre laser (2 MHz repetition rate) operating in a regime between stable and noise-like emission^{15,75}. These single-shot measurements show that the laser spectrum unpredictably collapses into a structured form and rapidly returns to its original soliton profile^{15,75}.

Direct observation of transient rare phenomena has enhanced theoretical understanding of stochastically driven nonlinear systems and spawned new ideas such as the generation of rogue waves^{76–80} (Fig. 4). In addition, time stretch has revealed shot-to-shot stochasticity and coherence in mode-locked lasers⁸¹ and observations of spectral dynamics during the onset of optical parametric oscillation⁸² (Fig. 4). Soliton molecules are complexes formed by attractive and repulsive forces mediated by the propagation environment. They are another fascinating manifestation of stochastically driven nonlinear systems^{16,83–86}.

There are yet other examples of intriguing non-stationary soliton dynamics that can be studied such as the rains of solitons^{87,88}. Initial observation of these solitons in mode-locked fibre lasers was through a few frames of intensity dynamics measured at different times. Later, the rains of solitons phenomenon was demonstrated in fibre lasers with different gain mechanisms⁸⁹, with different cavity configurations⁹⁰ and with different saturable absorbers⁹¹.

Recently, it has been experimentally found that collections of both dark and grey solitons can be generated in fibre lasers during the onset of noise-like lasing⁹² and in various modes of operation of a passively mode-locked laser^{93,94}. Mutual dynamics of dark and bright coherent structures result in distinctive features on the noise-like envelope of the main pulse, making its properties difficult to access in the pure temporal domain with conventional techniques.

Relativistic electron beam diagnostics. One of the remarkable applications of time stretch is in particle accelerators. In a milestone demonstration, the time-stretch ADC has been used to study electron-beam instability caused by the interaction between a relativistic electron bunch with its own electromagnetic field^{17,18}. This important effect is encountered in linear accelerators and synchrotron radiation

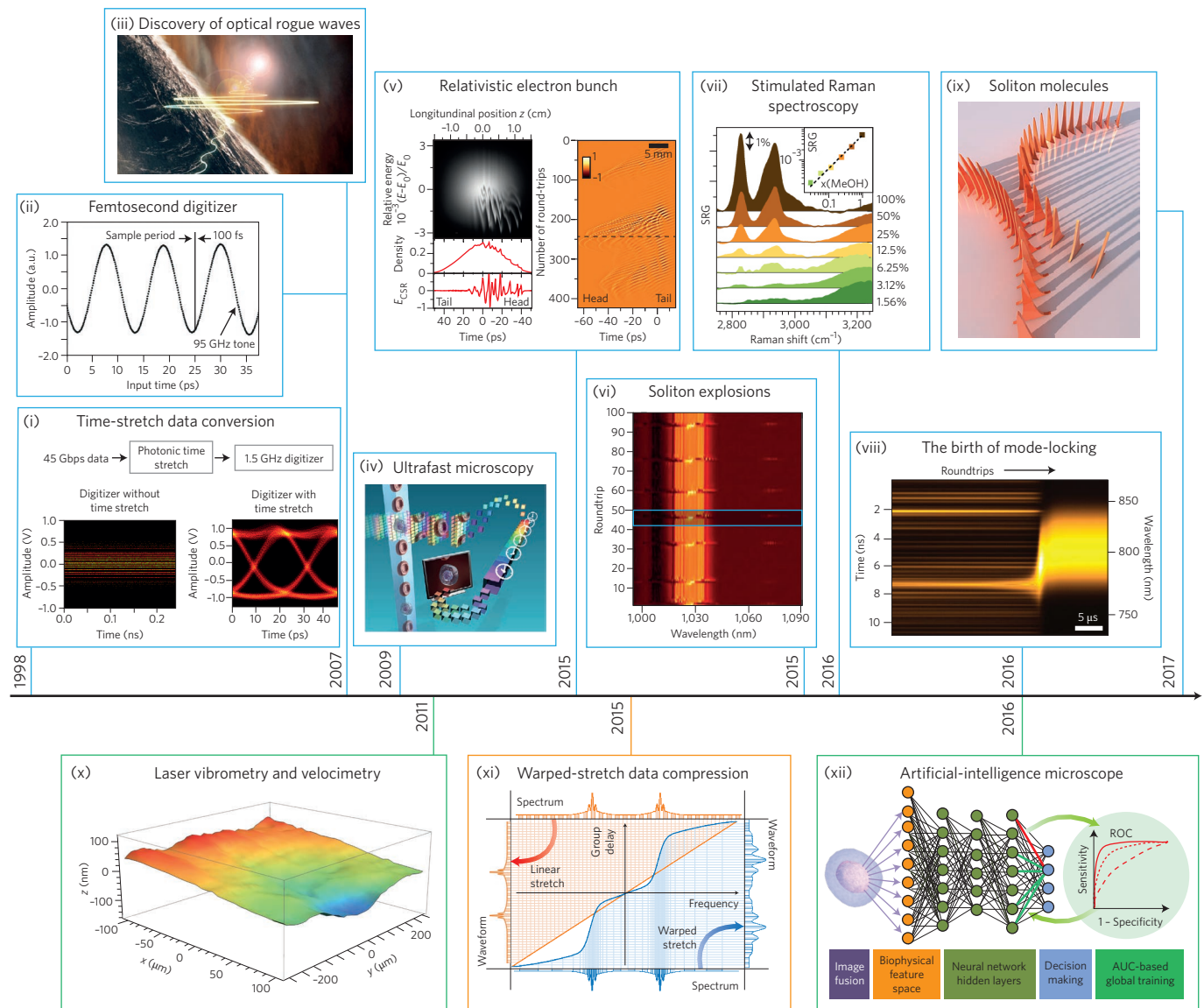


Figure 4 | Applications of time stretch. Blue: photonic time stretch was initially developed to overcome the speed and resolution limitations of high-speed ADCs¹² (i) leading to the development of a femtosecond digitizer²⁹ (ii), and later became the foundation of many ultrafast instrumentation techniques in spectroscopy, for example stimulated Raman spectroscopy^{19,20} (vii), imaging and microscopy³⁰ (iv), and in the observation of relativistic¹⁷ (v) and nonlinear dynamics for example optical rogue waves⁵ (iii), soliton explosions¹⁵ (vi), build-up of mode-locking²³ (viii), and internal dynamics of soliton molecules¹⁶ (ix). Green: the coherent (full-field) version, which uses phase measurement using interferometry or phase retrieval algorithms to recover the phase of the optical pulses, has enabled record-breaking instruments in laser vibrometry and velocimetry³¹ (x), quantitative phase imaging and a time-stretch microscope augmented by artificial intelligence for label-free cell classification²² (xii). Orange: the new concept of warped time stretch is opening up opportunities in real-time optical data analytics and data compression^{26,27} (xi). Panel (i) shows an eye diagram of 45 Gbps data captured by a 1.5 GHz electronic digitizer after its speed was boosted by 34× using photonic time stretch³⁵. Figure adapted from: (i), ref. 35, (iv), ref. 124, Wiley; (ii), ref. 29, AIP Publishing LLC; (v), ref. 17, (xi), ref. 26, (xii), ref. 22, under a Creative Commons licence (<https://creativecommons.org/licenses/by/4.0/>); (vi), ref. 15, (vii), ref. 20, OSA; (viii), ref. 123, Macmillan Publishers Ltd; (ix), University of Goettingen; (x), ref. 125, SPIE.

sources and produces pulses of intense terahertz emission. The evolution of microscopic structures appearing within charged relativistic electron bunches was observed¹⁷.

There are two main types of accelerator: one is the linear accelerator where the electrons are accelerated and discarded shortly after; and the other is the storage ring in which the electrons go through a closed-loop trajectory and are stored over a long duration. Previous methods captured structures of electron bunches destructively and at low repetition rates (typically 10–60 Hz) by transversally deflecting the electrons and discarding them at a fluorescent screen⁹⁵. Owing

to their destructive nature, the use of these observation methods was limited to the linear accelerators. Time stretch enables non-destructive observation of electron bunches through direct measurements of their electromagnetic radiation fields, and therefore it can be used in storage rings, where the electron bunches need to be preserved. Furthermore, time stretch improves the observation rates by several orders of magnitude. Such vital quantitative measurements are expected to lead to new levels of understanding of electron-beam dynamics, validation of theoretical models, and creation of high-power sources of coherent radiation^{17,18}.

Warped stretch, spectrotemporal gearbox and optical data compression. By virtue of their high single-shot rates and continuous measurements, time-stretch instruments generate a torrent of data creating a big-data predicament. Serendipitously, new concepts based on warped-stretch transformation are emerging that can potentially solve this problem. These transformations enable the engineering of the time–bandwidth product of the information carried by an optical carrier²³, a discovery that runs counter to expectation that linear processes conserve the time–bandwidth product. Warped-stretch transformations are implemented using frequency-dependent group delay; a process nonlinear in frequency but linear in amplitude. While (amplitude) linear processes do indeed conserve the time–bandwidth product of the carrier, they do not exclude modification of the envelope's time–bandwidth product. The warped reshaping prior to analog-to-digital conversion solves the fundamental problem with Nyquist sampling of frequencies above the Nyquist rate being undersampled and those below being oversampled. Warped stretch solves this problem by causing non-uniform Fourier domain sampling, where the sampling rate self-adapts to the local information content (local entropy) of signals, leading to more efficient utilization of samples^{23,28,96}. The function of warped time stretching is analogous to mechanical gearboxes with automatic gear ratios^{28,40}.

To implement arbitrary frequency-dependent group delay dispersions, the phase profile of the dispersive device is expanded in terms of basis functions²⁸. These basis sets can be viewed as a series of cascaded group delay operations each performing primitive stretch operations. Nonlinear group delay modes have been introduced as primitive building blocks for complex warped-stretch transformations (Box 2). In addition to non-uniform Fourier domain sampling for data compression, a subset of stretch primitives with proper symmetry can perform edge and event detection²⁸. For the case of data compression, digital reconstruction is not lossless. The reconstruction quality depends on the signal-to-noise ratio of the signal, and the amount of information loss is predominantly limited by the dynamic range (the effective number of bits (ENOB)) of the ADC used⁹⁶.

Imaging and cancer detection. In time-stretch imaging^{30,97}, the object's spatial information is encoded in the spectrum of laser pulses within a short (picoseconds) pulse duration. Each pulse representing one frame of the camera is then stretched in time so that it can be digitized in real time by an ADC. With a shutter speed (illumination) in the picosecond range, the camera freezes the motion of objects travelling at high velocity to achieve blur-free imaging. The frame rate is the same as the laser pulse repetition rate and reaches billion images per second⁹⁸. Detection sensitivity is challenged by the low number of photons collected during the ultrashort shutter time (optical pulse width) and the drop in the peak optical power resulting from the time stretch. These issues are solved with amplified time stretch that implements a Raman amplifier within the dispersive device for simultaneous amplification and stretching. In the coherent version of the instrument³¹, the time-stretch imaging is combined with spectral interferometry to produce quantitative phase and intensity images in real time and at high throughput.

To address the big-data problem arising in such a high-frame-rate imaging modality, the warped-stretch transform has been used to achieve non-uniform spatial resolution leading to optical image compression²⁷. This bioinspired method emulates the function of the fovea centralis in the retina of the human eye to offer high resolution in the central field of view and lower resolution in the peripheral vision²⁸. It is important to note that this foveated sampling is achieved not by varying the sampling rate, but by warping the signal prior to fixed-rate sampling.

Integrated with a microfluidic channel, a coherent time-stretch imaging system captures quantitative phase and intensity images of particles or individual cells in flow. In this fashion, the system acts as a high-speed imaging flow cytometer with cell flow rates as high as

10 m s⁻¹, reaching up to 100,000 cells s⁻¹ throughput. The information of quantitative optical loss and phase images are fused and transformed into biophysical features and analysed using artificial-intelligence algorithms, leading to record label-free classification accuracy of 96%²².

Spatiotemporal dynamics. In laser cavities, non-stationary behaviour occurs over two distinct timescales. 'Fast time' is the intrapulse timescale corresponding to the structure within each pulse. 'Slow time' is the number of round trips and is the timescale over which pulse-to-pulse fluctuations occur.

For many dynamical and transient phenomena, the same pulse has to be observed over many consecutive cavity round-trips to capture events such as soliton explosions. Light evolution in a cavity has an inherent cyclic spatiotemporal nature, that is, radiation is propagating through the cavity and changing its properties from one round trip to another. In other words, the temporal characteristics of the radiation change in space during propagation along the laser cavity. Visualizing the spatiotemporal dynamics provides useful insights into the internal structure and properties of laser radiation, including the appearance and precursors of rare non-repetitive structures. The term spatio refers to the axial dimension in the laser cavity.

Studying lasers as systems generating multiple spatiotemporal regimes has led to the observation of previously unknown mechanisms of light generation with links to other fields of physics. In particular, it was found that a quasi-continuous-wave (quasi-CW) fibre laser could generate a large number of strongly correlated modes with highly suppressed intensity fluctuations, in sharp contrast to more typical operation with greatly pronounced fluctuations. Such systems exhibit a laminar–turbulent transition similar to that seen in fluid flows⁹⁹. Optical wave turbulence in quasi-CW lasers has a variety of well-distinguished spatiotemporal fingerprints¹⁰⁰ that can be used to characterize the system. A similar transition is found theoretically using the complex Ginzburg–Landau model of a mode-locked laser¹⁰¹.

Mode-locked fibre lasers offer even larger variety of temporal operational regimes that depend on pump power and mode-locking settings. In passively mode-locked fibre lasers, alongside conventional stable single-pulse operation, much more complex dynamics with noise-like pulses has been observed^{29,102–106}. While in the temporal domain such pulses might have a complex and rather irregular structure making it difficult to classify and study them, distinct and steady-state generation regimes are revealed in the spatiotemporal domain⁹³.

Experimental access to the additional degree of freedom offered by the time-stretch technique, both fast and slow dynamics over cavity round-trips, offers new possibilities to tailor and control the lasing. Advanced applications such as high-performance micromachining and ablation¹⁰⁷ rely not only on the properties of each individual pulse, but also on mutual dynamics of the pulses over a slow evolution scale. Spatiotemporal generation regimes could be controlled in real time by prescribing a set of cavity parameters, for example by means of evolutionary algorithms¹⁰⁸.

Besides the distinct spatiotemporal generation regimes, the ability to experimentally assess intensity both over the temporal and spatial coordinate opens up new possibilities to study emerging coherent structures. Dissipative rogue waves can be generated via bunching of structures within a noise-like pulse^{109,110}. Similarly, when looking at the spatiotemporal dynamics of a quasi-CW fibre laser¹¹¹, researchers made the first observation of polarization rogue-waves. Other types of optical rogue wave have been recently identified as aperiodically generated spatiotemporal structures: dark three-sister rogue waves¹¹² and waves emerging from the interaction of three pulses having different group velocities^{113,114}.

Future perspectives

Beam diagnostics in particle accelerators, such as the recently demonstrated measurement of relativistic electron beam structure using

the time-stretch ADC¹⁷, represents an extremely challenging but high-impact application for single-shot measurement techniques. Utilities include advanced diagnostics during machine development to beam-performance monitoring during regular operation¹¹⁵. In addition to the wideband ADC for data capture, sensors based on interaction of the beam with light are also essential. Going forward, advances in instrumentation will enable observations of new physical phenomena with potential translation into practical applications such as sources of coherent radiation.

An important class of optical instruments are those based on Mie and Rayleigh scattering of light for measuring the morphological features of particles. Light scattering is the basis of flow cytometers, which are the workhorse of the blood-testing industry¹¹⁶. By combining time stretch with spectrum-to-angle-encoded illumination, a new class of dynamic light scattering instruments can be created that feature higher dynamic range with faster acquisition¹¹⁷. This type of instrument captures the complete angular spectrum of light scattered by a particle using a single detector without the need for mechanical scanning. By shaping the power spectral density of the illuminating pulse, it compensates for lower power at large scattering angles, thereby equalizing the angular spectrum¹¹⁷. In the future, application of time stretch to light scattering measurements can create new medical and industrial applications for this important optical phenomenon.

A rarely explored application of time-stretch spectroscopy is in fast interrogation of fibre Bragg grating sensors¹¹⁸. Such sensors are able to measure strain, temperature and, when functionalized, chemical and biochemical changes in their environment. Being optics based, they can be placed in harsh environments and interrogated from a remote location in power plants, engines, motors, dams and bridges. The high-speed nature of time-stretch spectroscopy will enable multiplexed and fast real-time monitoring of a large number of distributed sensors networks for structural health monitoring. A more challenging but impactful future direction is direct measurement of optical spectra during combustion for optimization of output power and efficiency.

Recently, there has been renewed interest in optical computing. The concept has been reintroduced as an analog engine able to serve as a specialized processor to augment digital electronic computers¹¹⁹. This approach exploits the fact that dynamical processes occur much faster in optical systems than can be simulated with a digital computer. An analog optical computer based on nonlinear dynamics in a photonic medium will be orders-of-magnitude faster in exploration of nonlinear phenomena. However, these rapid dynamics must be observed as they unfold in real time and, to detect transient events, measurements must span long intervals. Time-stretch instruments are the ideal output device for such analog optical computers.

Moving forward, one area where innovations are needed is in dealing with the massive amount of data generated by high-frame-rate real-time instruments and metrology equipment. Some of the technologies that will be needed include data compression, digital processing and machine learning. Recent progress in this area has come from generalization of time stretch to nonlinear stretch and full-field optical detection^{23,26,28}. In such systems, the dispersion profile is designed based on the known spectral sparsity of the data²⁶. Warped spectrum-to-time mapping enables real-time spectroscopy with non-uniform (foveated) spectral resolutions, pinpointing the spectral features at specific wavelengths. In this context, it has been recently shown that warped-stretch transformations will also lead to improved signal-to-noise ratio compared with linear stretch, leading to higher sensitivity of the instrument²⁸. The optical data compression capabilities enabled by these transforms²⁷ further push the boundaries of data acquisition rate and record length, attributes that are critical in the study of nonlinear dynamics in photonic and electronic systems. In the context of

Box 3 | Time stretch in computational imaging.

The Phase Stretch Transform is a computational algorithm inspired by the physics of photonic time stretch. While it can also be implemented in the analog domain to detect transitions and events in temporal waveforms, its biggest impact may be in computational imaging for feature detection and super-resolution imaging. Emulating the physics of group velocity dispersion, but in two-dimensional space, the algorithm applies a frequency-dependent nonlinear phase kernel, $\tilde{K}[u,v]$, to the two-dimensional Fourier transform of the image, $\text{FFT}^2\{E_i[x,y]\}$, and uses the phase of the spatial output to locate the edges¹²⁰ as well as to improve the point spread function for super-resolution imaging¹²¹:

$$\text{PST}\{E_i[x,y]\} \triangleq \angle\{\text{IFFT}^2\{\text{FFT}^2\{E_i[x,y]\} \times \tilde{K}[u,v] \times \tilde{L}[u,v]\}\}$$

where FFT is the fast Fourier transform and IFFT is the inverse FFT. In detection of fast transitions, corners and edges (image), high-frequency components receive a larger phase shift from the phase kernel $\tilde{K}[u,v]$ compared with the low-frequency elements and become emphasized. A localization kernel, $\tilde{L}[u,v]$, can be employed to apply the phase kernel to only a range of spatial frequencies in order to ignore highly local variations such as speckle noise. The features identified by the Phase Stretch Transform are used in an image recognition or computer vision pipeline, and the kernel parameters can be adaptively adjusted by the artificial-intelligence algorithms. (The Matlab code for the Phase Stretch Transform is available on Github.)



Feature detection and resolution enhancement by the Phase Stretch Transform. Digital implementation of the Phase Stretch Transform in two-dimensional spatial domain^{120,121}. Here, an astronomical image (left) and its Phase Stretch Transform (right) are shown. The transform unveils hidden features and improves the image quality with applications to super-resolution microscopy¹²¹. Left panel: NASA Ames Research Center / Brian Day.

photonics, time-stretch spectral shearing interferometry (Box 2) presents a fertile ground for expanding the full-field characterization capabilities.

Research on the physics of time stretch has led to the creation of a new class of image-processing algorithms. Implemented in the numerical domain and extended to two dimensions, digital emulation of the optical physics inherent in group delay dispersion has shown several applications in digital image processing^{120,121}. One realization of this is the Phase Stretch Transform that has already proven utility in computational imaging (Box 3). Although in its infancy, this area of research is poised to have applications in machine vision via artificial intelligence.

Received 22 September 2016; accepted 21 April 2017;
published online 1 June 2017

References

- Jalali, B., Solli, D., Goda, K., Tsia, K. & Ropers, C. Real-time measurements, rare events and photon economics. *Eur. Phys. J. Special Topics* **185**, 145–157 (2010).
- Taleb, N. N. *The Black Swan: The Impact of the Highly Improbable* (Random House, 2007).
- VanderLugt, A. *Optical Signal Processing* (Wiley, 2005).
- Boyratz, O. & Jalali, B. Demonstration of a silicon Raman laser. *Opt. Express* **12**, 5269–5273 (2004).
- Solli, D., Ropers, C., Koonath, P. & Jalali, B. Optical rogue waves. *Nature* **450**, 1054–1057 (2007).
- Akhmediev, N., Ankiewicz, A. & Taki, M. Waves that appear from nowhere and disappear without a trace. *Phys. Lett. A* **373**, 675–678 (2009).
- Pisarchik, A. N., Jaimes-Reategui, R., Sevilla-Escoboza, R., Huerta-Cuellar, G. & Taki, M. Rogue waves in a multistable system. *Phys. Rev. Lett.* **107**, 274101 (2011).
- Dudley, J. M., Dias, F., Erkintalo, M. & Genty, G. Instabilities, breathers and rogue waves in optics. *Nat. Photon.* **8**, 755–764 (2014).
- Akhmediev, N. *et al.* Roadmap on optical rogue waves and extreme events. *J. Opt.* **18**, 063001 (2016).
- Suret, P. *et al.* Single-shot observation of optical rogue waves in integrable turbulence using time microscopy. *Nat. Commun.* **7**, 13136 (2016).
- Mahjoubfar, A., Goda, K., Betts, G. & Jalali, B. Optically amplified detection for biomedical sensing and imaging. *J. Opt. Soc. Am. A* **30**, 2124–2132 (2013).
- Bhushan, A., Coppinger, F. & Jalali, B. Time-stretched analogue-to-digital conversion. *Electron. Lett.* **34**, 1081–1082 (1998).
- Coppinger, F., Bhushan, A. & Jalali, B. Photonic time stretch and its application to analog-to-digital conversion. *IEEE Trans. Microwave Theory Techniques* **47**, 1309–1314 (1999).
- Jalali, B. & Coppinger, F. M. A. Data conversion using time manipulation. US patent US6288659 (2001).
- Runge, A. F., Broderick, N. G. & Erkintalo, M. Observation of soliton explosions in a passively mode-locked fiber laser. *Optica* **2**, 36–39 (2015).
- Herink, G., Kurtz, F., Jalali, B., Solli, D. & Ropers, C. Real-time spectral interferometry probes the internal dynamics of femtosecond soliton molecules. *Science* **356**, 50–54 (2017).
- Roussel, E. *et al.* Observing microscopic structures of a relativistic object using a time-stretch strategy. *Sci. Rep.* **5**, 10330 (2015).
- Evain, C. *et al.* Direct observation of spatiotemporal dynamics of short electron bunches in storage rings. *Phys. Rev. Lett.* **118**, 054801 (2017).
- Solli, D., Chou, J. & Jalali, B. Amplified wavelength-time transformation for real-time spectroscopy. *Nat. Photon.* **2**, 48–51 (2008).
- Saltarelli, F. *et al.* Broadband stimulated Raman scattering spectroscopy by a photonic time stretcher. *Opt. Express* **24**, 21264–21275 (2016).
- Dobner, S. & Fallnich, C. Dispersive Fourier transformation femtosecond stimulated Raman scattering. *Appl. Phys. B* **122**, 278 (2016).
- Chen, C. L. *et al.* Deep learning in label-free cell classification. *Sci. Rep.* **6**, 21471 (2016).
- Jalali, B., Chan, J. & Asghari, M. H. Time-bandwidth engineering. *Optica* **1**, 23–31 (2014).
- Chan, J. C., Mahjoubfar, A., Chen, C. L. & Jalali, B. Context-aware image compression. *PLoS ONE* **11**, e0158201 (2016).
- Asghari, M. H. & Jalali, B. Anamorphic transformation and its application to time-bandwidth compression. *Appl. Opt.* **52**, 6735–6743 (2013).
- Mahjoubfar, A., Chen, C. L. & Jalali, B. Design of warped stretch transform. *Sci. Rep.* **5**, 17148 (2015).
- Chen, C. L., Mahjoubfar, A. & Jalali, B. Optical data compression in time stretch imaging. *PLoS ONE* **10**, e0125106 (2015).
- Jalali, B. & Mahjoubfar, A. Tailoring wideband signals with a photonic hardware accelerator. *Proc. IEEE* **103**, 1071–1086 (2015).
- Chou, J., Boyraz, O., Solli, D. & Jalali, B. Femtosecond real-time single-shot digitizer. *Appl. Phys. Lett.* **91**, 161105 (2007).
- Goda, K., Tsia, K. & Jalali, B. Serial time-encoded amplified imaging for real-time observation of fast dynamic phenomena. *Nature* **458**, 1145–1149 (2009).
- Mahjoubfar, A. *et al.* High-speed nanometer-resolved imaging vibrometer and velocimeter. *Appl. Phys. Lett.* **98**, 101107 (2011).
- Wong, T. T., Lau, A. K., Wong, K. K. & Tsia, K. K. Optical time-stretch confocal microscopy at 1 μm . *Opt. Lett.* **37**, 3330–3332 (2012).
- Bosworth, B. T. *et al.* High-speed flow microscopy using compressed sensing with ultrafast laser pulses. *Opt. Express* **23**, 10521–10532 (2015).
- Han, Y. & Jalali, B. Photonic time-stretched analog-to-digital converter: fundamental concepts and practical considerations. *J. Lightwave Technol.* **21**, 3085–3103 (2003).
- Fard, A. M., Gupta, S. & Jalali, B. Photonic time-stretch digitizer and its extension to real-time spectroscopy and imaging. *Laser Photon. Rev.* **7**, 207–263 (2013).
- Kim, J., Park, M. J., Perrott, M. H. & Kärtner, F. X. Photonic subsampling analog-to-digital conversion of microwave signals at 40-GHz with higher than 7-ENOB resolution. *Opt. Express* **16**, 16509–16515 (2008).
- Konishi, T., Tanimura, K., Asano, K., Oshita, Y. & Ichioka, Y. All-optical analog-to-digital converter by use of self-frequency shifting in fiber and a pulse-shaping technique. *J. Opt. Soc. Am. B* **19**, 2817–2823 (2002).
- Portuondo-Campa, E., Paschotta, R. & Lecomte, S. Sub-100 attosecond timing jitter from low-noise passively mode-locked solid-state laser at telecom wavelength. *Opt. Lett.* **38**, 2650–2653 (2013).
- Lonappan, C. K., Madni, A. M. & Jalali, B. Single-shot network analyzer for extremely fast measurements. *Appl. Optics* **55**, 8406–8412 (2016).
- Jalali, B., Chan, J. & Mahjoubfar, A. Analog gearbox: a photonic hardware accelerator. In *Avionics Vehicle Fiber-Optics Photon. Conf. (AVFOP)* 1–2 (IEEE, 2016).
- Yegnanarayanan, S., Trinh, P. & Jalali, B. Recirculating photonic filter: a wavelength-selective time delay for phased-array antennas and wavelength code-division multiple access. *Opt. Lett.* **21**, 740–742 (1996).
- Solli, D., Gupta, S. & Jalali, B. Optical phase recovery in the dispersive Fourier transform. *Appl. Phys. Lett.* **95**, 231108 (2009).
- Buckley, B. W., Madni, A. M. & Jalali, B. Coherent time-stretch transformation for real-time capture of wideband signals. *Opt. Express* **21**, 21618–21627 (2013).
- Trebino, R. *et al.* Measuring ultrashort laser pulses in the time-frequency domain using frequency-resolved optical gating. *Rev. Sci. Instrum.* **68**, 3277–3295 (1997).
- Iaconis, C. & Walmsley, I. A. Spectral phase interferometry for direct electric-field reconstruction of ultrashort optical pulses. *Opt. Lett.* **23**, 792–794 (1998).
- Konishi, T., Kato, T. & Goto, H. Waveform reconstruction device, waveform reconstruction system, and waveform reconstruction method. US patent US8886037 (2014).
- DeVore, P. T., Buckley, B. W., Asghari, M. H., Solli, D. R. & Jalali, B. Coherent time-stretch transform for near-field spectroscopy. *IEEE Photon. J.* **6**, 1–7 (2014).
- Mahjoubfar, A., Chen, C., Niazi, K. R., Rabizadeh, S. & Jalali, B. Label-free high-throughput cell screening in flow. *Biomed. Opt. Express* **4**, 1618–1625 (2013).
- Han, Y. & Jalali, B. Continuous-time time-stretched analog-to-digital converter array implemented using virtual time gating. *IEEE Trans. Circuits Systems I: Regular Papers* **52**, 1502–1507 (2005).
- Chou, J., Conway, J. A., Seifler, G. A., Valley, G. C. & Jalali, B. Photonic bandwidth compression front end for digital oscilloscopes. *J. Lightwave Technol.* **27**, 5073–5077 (2009).
- Ng, W., Rockwood, T., Seifler, G. & Valley, G. Demonstration of a large stretch-ratio photonic analog-to-digital converter with 8 ENOB for an input signal bandwidth of 10 GHz. *IEEE Photon. Technol. Lett.* **24**, 1185–1187 (2012).
- Wong, J. H. *et al.* Photonic time-stretched analog-to-digital converter amenable to continuous-time operation based on polarization modulation with balanced detection scheme. *J. Lightwave Technol.* **29**, 3099–3106 (2011).
- Valley, G. C. Photonic analog-to-digital converters. *Opt. Express* **15**, 1955–1982 (2007).
- Stigwall, J. & Galt, S. Signal reconstruction by phase retrieval and optical backpropagation in phase-diverse photonic time-stretch systems. *J. Lightwave Technol.* **25**, 3017–3027 (2007).
- Han, Y., Boyraz, O. & Jalali, B. Ultrawide-band photonic time-stretch A/D converter employing phase diversity. *IEEE Trans. Microwave Theory Techniques* **53**, 1404–1408 (2005).
- Fuster, J., Novak, D., Nirmalathas, A. & Marti, J. Single-sideband modulation in photonic time-stretch analogue-to-digital conversion. *Electron. Lett.* **37**, 67–68 (2001).
- Fard, A. *et al.* All-optical time-stretch digitizer. *Appl. Phys. Lett.* **101**, 051113 (2012).
- Lonappan, C. K. *et al.* Time-stretch accelerated processor for real-time, in-service, signal analysis. In *IEEE Global Conf. Signal Information Processing* 707–711 (2014).
- Kitayama, K.-I. & Wada, N. Photonic IP routing. *IEEE Photon. Technol. Lett.* **11**, 1689–1691 (1999).
- Wada, N. & Kitayama, K.-I. A 10 gb/s optical code division multiplexing using 8-chip optical bipolar code and coherent detection. *J. Lightwave Technol.* **17**, 1758–1765 (1999).
- Ruban, V. *et al.* Rogue waves—towards a unifying concept?: Discussions and debates. *Eur. Phys. J. Special Topics* **185**, 5–15 (2010).
- Wetzel, B. *et al.* Real-time full bandwidth measurement of spectral noise in supercontinuum generation. *Sci. Rep.* **2**, 882 (2012).
- Solli, D., Herink, G., Jalali, B. & Ropers, C. Fluctuations and correlations in modulation instability. *Nat. Photon.* **6**, 463–468 (2012).
- Godin, T. *et al.* Real time noise and wavelength correlations in octave-spanning supercontinuum generation. *Opt. Express* **21**, 18452–18460 (2013).
- Dean, R. in *Water Wave Kinematics* 609–612 (Springer, 1990).
- Kharif, C. & Pelinovsky, E. Physical mechanisms of the rogue wave phenomenon. *Eur. J. Mech. B* **22**, 603–634 (2003).

67. Gabaix, X., Gopikrishnan, P., Plerou, V. & Stanley, H. E. A theory of power-law distributions in financial market fluctuations. *Nature* **423**, 267–270 (2003).
68. Anderson, C. *The Long Tail: Why the Future of Business is Selling Less of More* (Hachette Books, 2006).
69. Clauset, A., Shalizi, C. R. & Newman, M. E. Power-law distributions in empirical data. *SIAM Rev.* **51**, 661–703 (2009).
70. Pisarenko, V. & Rodkin, M. *Heavy-Tailed Distributions in Disaster Analysis* (Springer Science & Business Media, 2010).
71. Zhen-Ya, Y. Financial rogue waves. *Commun. Theor. Phys.* **54**, 947–949 (2010).
72. Birkholz, S., Brée, C., Demircan, A. & Steinmeyer, G. Predictability of rogue events. *Phys. Rev. Lett.* **114**, 213901 (2015).
73. Cundiff, S. T., Soto-Crespo, J. M. & Akhmediev, N. Experimental evidence for soliton explosions. *Phys. Rev. Lett.* **88**, 073903 (2002).
74. Soto-Crespo, J. M., Akhmediev, N. & Ankiewicz, A. Pulsating, creeping, and erupting solitons in dissipative systems. *Phys. Rev. Lett.* **85**, 2937–2940 (2000).
75. Runge, A. F., Broderick, N. G. & Erkintalo, M. Dynamics of soliton explosions in passively mode-locked fiber lasers. *J. Opt. Soc. Am. B* **33**, 46–53 (2016).
76. Akhmediev, N., Dudley, J. M., Solli, D. & Turitsyn, S. Recent progress in investigating optical rogue waves. *J. Opt.* **15**, 060201 (2013).
77. Liu, Z., Zhang, S. & Wise, F. W. Rogue waves in a normal-dispersion fiber laser. *Opt. Lett.* **40**, 1366–1369 (2015).
78. Lecaplain, C. & Grellu, P. Rogue waves among noise-like-pulse laser emission: an experimental investigation. *Phys. Rev. A* **90**, 013805 (2014).
79. Runge, A. F., Agueraray, C., Broderick, N. G. & Erkintalo, M. Coherence and shot-to-shot spectral fluctuations in noise-like ultrafast fiber lasers. *Opt. Lett.* **38**, 4327–4330 (2013).
80. Solli, D. R., Ropers, C. & Jalali, B. Active control of rogue waves for stimulated supercontinuum generation. *Phys. Rev. Lett.* **101**, 233902 (2008).
81. Runge, A. F., Agueraray, C., Broderick, N. G. & Erkintalo, M. Raman rogue waves in a partially mode-locked fiber laser. *Opt. Lett.* **39**, 319–322 (2014).
82. Descloux, D. *et al.* Spectrotemporal dynamics of a picosecond OPO based on chirped quasi-phase-matching. *Opt. Lett.* **40**, 280–283 (2015).
83. Akhmediev, N., Ankiewicz, A. & Soto-Crespo, J. Multisoliton solutions of the complex Ginzburg–Landau equation. *Phys. Rev. Lett.* **79**, 4047–4051 (1997).
84. Ortaç, B. *et al.* Observation of soliton molecules with independently evolving phase in a mode-locked fiber laser. *Opt. Lett.* **35**, 1578–1580 (2010).
85. Soto-Crespo, J. M., Grellu, P., Akhmediev, N. & Devine, N. Soliton complexes in dissipative systems: vibrating, shaking, and mixed soliton pairs. *Phys. Rev. E* **75**, 016613 (2007).
86. Chen, W.-C., Chen, G.-J., Han, D.-A. & Li, B. Different temporal patterns of vector soliton bunching induced by polarization-dependent saturable absorber. *Opt. Fiber Technol.* **20**, 199–207 (2014).
87. Chouli, S. & Grellu, P. Soliton rains in a fiber laser: an experimental study. *Phys. Rev. A* **81**, 063829 (2010).
88. Chouli, S. & Grellu, P. Rains of solitons in a fiber laser. *Opt. Express* **17**, 11776–11781 (2009).
89. Bao, C., Xiao, X. & Yang, C. Soliton rains in a normal dispersion fiber laser with dual-filter. *Opt. Lett.* **38**, 1875–1877 (2013).
90. Niang, A., Amrani, F., Salhi, M., Grellu, P. & Sanchez, F. Rains of solitons in a figure-of-eight passively mode-locked fiber laser. *Appl. Phys. B* **116**, 771–775 (2014).
91. Huang, S. *et al.* Soliton rains in a graphene-oxide passively mode-locked ytterbium-doped fiber laser with all-normal dispersion. *Laser Phys. Lett.* **11**, 025102 (2013).
92. Kelleher, E. & Travers, J. Chirped pulse formation dynamics in ultra-long mode-locked fiber lasers. *Opt. Lett.* **39**, 1398–1401 (2014).
93. Churkin, D. *et al.* Stochasticity, periodicity and localized light structures in partially mode-locked fibre lasers. *Nat. Commun.* **6**, 7004 (2015).
94. Donovan, G. M. Dynamics and statistics of noise-like pulses in modelocked lasers. *Physica D* **309**, 1–8 (2015).
95. Krejčík, P. *et al.* Commissioning the new LCLS X-band transverse deflecting cavity with femtosecond resolution. In *Proc. Int. Beam Instrumentation Conf.* 308–311 (2013).
96. Chan, J., Mahjoubfar, A., Asghari, M. & Jalali, B. Reconstruction in time-bandwidth compression systems. *Appl. Phys. Lett.* **105**, 221105 (2014).
97. Goda, K. *et al.* High-throughput single-microparticle imaging flow analyzer. *Proc. Natl Acad. Sci. USA* **109**, 11630–11635 (2012).
98. Xing, F. *et al.* A 2-GHz discrete-spectrum waveband-division microscopic imaging system. *Opt. Commun.* **338**, 22–26 (2015).
99. Avila, K. *et al.* The onset of turbulence in pipe flow. *Science* **333**, 192–196 (2011).
100. Tarasov, N., Sugavanam, S. & Churkin, D. Spatio-temporal generation regimes in quasi-CW Raman fiber lasers. *Opt. Express* **23**, 24189–24194 (2015).
101. Wabnitz, S. Optical turbulence in fiber lasers. *Opt. Lett.* **39**, 1362–1365 (2014).
102. Horowitz, M. & Silberberg, Y. Control of noise-like pulse generation in erbium-doped fiber lasers. *IEEE Photon. Technol. Lett.* **10**, 1389–1391 (1998).
103. Zhao, L., Tang, D., Cheng, T., Tam, H. & Lu, C. 120nm bandwidth noise-like pulse generation in an erbium-doped fiber laser. *Opt. Commun.* **281**, 157–161 (2008).
104. Kobtsev, S., Kukarin, S., Smirnov, S., Turitsyn, S. & Latkin, A. Generation of double-scale femto/pico-second optical lumps in mode-locked fiber lasers. *Opt. Express* **17**, 20707–20713 (2009).
105. North, T. & Rochette, M. Raman-induced noise-like pulses in a highly nonlinear and dispersive all-fiber ring laser. *Opt. Lett.* **38**, 890–892 (2013).
106. Suzuki, M., Ganeev, R. A., Yoneya, S. & Kuroda, H. Generation of broadband noise-like pulse from Yb-doped fiber laser ring cavity. *Opt. Lett.* **40**, 804–807 (2015).
107. Kalaycıoğlu, H., Akçaalan, Ö., Yavaş, S., Eldeniz, Y. & İlday, F. Burst-mode Yb-doped fiber amplifier system optimized for low-repetition-rate operation. *J. Opt. Soc. Am. B* **32**, 900–906 (2015).
108. Andral, U. *et al.* Fiber laser mode locked through an evolutionary algorithm. *Optica* **2**, 275–278 (2015).
109. Lecaplain, C., Grellu, P., Soto-Crespo, J. & Akhmediev, N. Dissipative rogue waves generated by chaotic pulse bunching in a mode-locked laser. *Phys. Rev. Lett.* **108**, 233901 (2012).
110. Liu, M. *et al.* Dissipative rogue waves induced by long-range chaotic multi-pulse interactions in a fiber laser with a topological insulator-deposited microfiber photonic device. *Opt. Lett.* **40**, 4767–4770 (2015).
111. Sugavanam, S., Tarasov, N., Wabnitz, S. & Churkin, D. V. Ginzburg–Landau turbulence in quasi-CW Raman fiber lasers. *Laser Photon. Rev.* **9**, L35–L39 (2015).
112. Chen, S., Soto-Crespo, J. M. & Grellu, P. Dark three-sister rogue waves in normally dispersive optical fibers with random birefringence. *Opt. Express* **22**, 27632–27642 (2014).
113. Chen, S., Soto-Crespo, J. M. & Grellu, P. Watch-hand-like optical rogue waves in three-wave interactions. *Opt. Express* **23**, 349–359 (2015).
114. Chen, S. *et al.* Optical rogue waves in parametric three-wave mixing and coherent stimulated scattering. *Phys. Rev. A* **92**, 033847 (2015).
115. Raich, U. in *CAS CERN Accelerator School: Ion Sources* (ed. Bailey, R.) 503–514 (CERN, 2013).
116. Saeyns, Y., Van Gassen, S. & Lambrecht, B. N. Computational flow cytometry: helping to make sense of high-dimensional immunology data. *Nat. Rev. Immunol.* **16**, 449–462 (2016).
117. Adam, J., Mahjoubfar, A., Diebold, E. D., Buckley, B. W. & Jalali, B. Spectrally encoded angular light scattering. *Opt. Express* **21**, 28960–28967 (2013).
118. Lei, M., Zou, W., Li, X. & Chen, J. Ultrafast FBG interrogator based on time-stretch method. *IEEE Photon. Technol. Lett.* **28**, 778–781 (2016).
119. Solli, D. R. & Jalali, B. Analog optical computing. *Nat. Photon.* **9**, 704–706 (2015).
120. Asghari, M. H. & Jalali, B. Edge detection in digital images using dispersive phase stretch transform. *J. Biomed. Imaging* **2015**, 687819 (2015).
121. Ilovitsh, T., Jalali, B., Asghari, M. H. & Zalevsky, Z. Phase stretch transform for super-resolution localization microscopy. *Biomed. Opt. Express* **7**, 4198–4209 (2016).
122. Diebold, E. D. *et al.* Giant tunable optical dispersion using chromo-modal excitation of a multimode waveguide. *Opt. Express* **19**, 23809–23817 (2011).
123. Herink, G., Jalali, B., Ropers, C. & Solli, D. Resolving the build-up of femtosecond mode-locking with single-shot spectroscopy at 90 MHz frame rate. *Nat. Photon.* **10**, 321–326 (2016).
124. Jalali, B., Soon-Shiong, P. & Goda, K. Breaking speed and sensitivity limits: real-time diagnostics with serial time-encoded amplified microscopy. *Optik Photonik* **5**, 32–36 (2010).
125. Mahjoubfar, A. *et al.* 3D ultrafast laser scanner. *SPIE Proc.* **8611**, 86110N (2013).
126. Goda, K., Solli, D. R., Tsia, K. K. & Jalali, B. Theory of amplified dispersive Fourier transformation. *Phys. Rev. A* **80**, 043821 (2009).

Acknowledgements

We are grateful to S. Bielawski at Université des Sciences et Technologies de Lille, France for invaluable discussions on electron-beam diagnostics. We are also thankful to D. Solli at UCLA for helpful comments. The work at UCLA was partially supported by the Office of Naval Research (ONR) Multidisciplinary University Research Initiatives (MURI) on Optical Computing and by NantWorks, LLC.

Additional information

Reprints and permissions information is available online at www.nature.com/reprints. Publisher's note: Springer Nature remains neutral with regard to jurisdictional claims in published maps and institutional affiliations. Correspondence should be addressed to B.J.

Competing financial interests

B.J. is a co-founder of Time Photonics, the manufacturer of RogueScope, a single-shot spectrometer based on the time-stretch technique.